



Direct non-destructive trace and major elemental analysis in steel samples utilizing micro-focused bremsstrahlung radiation in X-ray fluorescence geometry

Kaushik Sanyal^{1,2} · Sangita Dhara^{1,2}

Received: 11 November 2021 / Accepted: 6 January 2022 / Published online: 7 March 2022
© The Author(s), under exclusive licence to The Japan Society for Analytical Chemistry 2022

Abstract

Stainless steel is a very important technological material used in various industries. In this work, a simple non-destructive method is developed for major as well as trace elemental determination in stainless steel samples using micro-X-ray fluorescence (XRF) based technique. The utilization of full bremsstrahlung excitation in combination with micro-focused geometry substantially reduces the detection limit of different elements present in stainless steel. The developed methodology is capable of determining elemental concentrations down to 30–80 ppm level in stainless steel matrix without any requirement of cumbersome dissolution or separation procedure. Elements such as Si, P, S and Co were determined simultaneously at trace level using the developed micro-XRF based technique. At the same time this technique is also capable of analyzing elements which are present at percentage levels. Till now there is no such report showing the capability of lab-XRF based non-destructive technique for the analysis of both major as well trace elements down to such low concentration level to the best of our knowledge. Moreover, the methodology involved is very simple and straight forward. The analytical results obtained were very much satisfactory with good accuracy and precision.

Keywords Nondestructive trace analysis · Steel sample · Micro-XRF · Bremsstrahlung radiation

Introduction

Stainless steel is a technologically important material. This material is widely used in different industries due to the presence of some crucial properties like high strength, corrosion resistance, hardness, etc. [1]. It is a necessary structural material for nuclear reactors used as cladding material in different types of reactors like fast breeder test reactor (FBTR) and prototype fast breeder reactor (PFBR) [2]. Different reactors use different types of steel because the structural as well as chemical properties of stainless steel are very much dependent on their chemical composition [3]. A slight change in the composition of steel can change its properties drastically. So a rapid, simple technique is required to

determine both trace as well as major elemental concentrations in these types of steel samples. Some of the conventional techniques available for the quantitative analysis of steel samples are inductively coupled plasma mass spectrometry (ICP-MS) [4], neutron activation analysis (NAA) [5, 6], spark-discharge optical emission spectroscopy (SD-OES) [7], etc. X-ray fluorescence (XRF) is another potential technique for the elemental analysis of steel samples. There are many advantageous features of XRF, like nondestructive analysis, multi-elemental analytical capability, fast measurement, simple instrumentation, wide elemental range, etc., which made this technique an ideal one for the elemental analysis in different types of matrices [8, 9]. Tiwari et.al had reported analysis of stainless steel samples using energy dispersive X-ray fluorescence (EDXRF) technique. However, they were not able to analyze elements like Si, P, S and Co which were present in trace amount, due to the limitation of instrumental sensitivity [10]. All the elements analyzed in that work were present in percentage level only. However, elements present at trace or ppm level have crucial role in determining the steel property. Si is generally used as de-oxidizer and it is present at around 1 wt% [11]. Presence of

✉ Kaushik Sanyal
ksanyal@barc.gov.in; kaushik.sanyal88@gmail.com

¹ Fuel Chemistry Division, Bhabha Atomic Research Centre, Mumbai 400085, India

² Homi Bhabha National Institute, Anushaktinagar, Mumbai 400094, India

excess Si in the steel sample may cause segregation of elements and formation of precipitates or low melting eutectics [12]. On the other hand P and S are very detrimental impurities which are present in ppm level. Therefore, it is also very important to analyze these elements as well along with major elements [13]. Total reflection X-ray fluorescence (TXRF) is another variant of XRF which has better sensitivity compared to EDXRF [14]. There are some reports of trace elemental analysis in steel samples using synchrotron radiation (SR) based TXRF technique [15]. However, in TXRF the sample has to be deposited in form of thin film specimen [16]. So the sample has to be dissolved before analysis. Moreover, separation of major matrix is also required in this method. So it is always better to develop a methodology which is direct, nondestructive, as well as simple with good sensitivity to determine both major as well as trace elemental concentrations in different types of steel samples. Micro-XRF is another variant of XRF which is generally used to determine the elemental homogeneity of different types of samples [17–20]. In lab based micro-XRF, a polycapillary focusing optics is required to obtain a fully focused beam. It was observed that the presence of micro-focused beam is very much beneficial to improve the detection limits [21]. Moreover, if the entire bremsstrahlung spectrum is used for the sample excitation, it will further improve the excitation efficiency as well as the detection limits, substantially [22]. In this work, we have assessed the possibility to utilize the advantageous features of micro-XRF geometry for the determination of trace as well as major elemental concentrations in more complex and important matrices like steel samples, nondestructively. There are some reports using hand held /lab based XRF spectrometers, where steel samples were analyzed non-destructively [23, 24]. However, they have reported elemental concentration in percentage level only. Previously, micro-XRF has been mostly used to determine elemental distribution or depth profiling. Recently, we have identified the potential- of micro-XRF geometry for trace analysis due to the presence of micro-focused beam and utilization of bremsstrahlung continuum, which substantially improved the detection limit and made it comparable with TXRF technique and sometimes better in some case [28]. We have not only reported the major elemental concentrations, but also the trace elemental concentrations which are present in ppm level in various types of steel samples, in a nondestructive manner in this study. This is a substantial improvement compared to the previously reported literature data where for determination of trace elements which are present in ppm level by XRF/TXRF; the sample was required to be dissolved and the major matrix was separated, which is very tedious and time consuming job [15].

In this manuscript, we have utilized the micro-XRF geometry to determine elements which are present in ppm to percent level in stainless steel samples, without any

dissolution or sample pre-treatment. This method will save a lot of time and effort. The details of this study are described in this paper.

Experimental

Materials used

During this experiment Standard Reference Materials (SRMs) numbered as 1151A, 1153A, 1154, 1295, 1297, and 1219 were used in form of disc having diameter of 34 mm and 19 mm thick. These SRMs basically represent the steel samples which are used in the industries such as SS 306, D9, etc. The composition of these standards is similar to the composition of industrial steels. The elements such as Si, Ti, V, Cr, Ni, Cu and Mo which are present in the industrial steels are present in these SRMs also. Hence, these SRMs were taken to prepare the calibration curves. Moreover, the Micro-XRF based methodology developed has to be validated with SRM. So, some industrial steel samples e.g. SS304, D9 alloy were also used for the validation purpose.

Micro-XRF spectrometer

The micro-XRF measurements in this study were performed by using ATI Micro-XRF scanning device. This micro-XRF consists of low power X-ray tube with Rh anode from Petrick GmbH [17]. This is an air cooled X-ray tube with Be window having a thickness of 100 μm . Voltage of 50 kV and current of 1 mA were chosen as the operating condition for the measurements. The X-ray beam is first emitted from the tube which has slit width (X) of 85 μm and length (Y) of 70 μm . The X-rays, after emitting from the tube, enters into a polycapillary optics (made by Fischer) that is directly attached with the X-ray tube. After several total reflections inside the polycapillary, the X-ray beam finally exit from the polycapillary and focused at a spot having size around 30 X 50 μm . A Peltier cooled SDD detector was used to detect the X-rays emitted from the sample. The active area of the detector is 30 mm^2 and sample to detector distance is 16 mm. There are two optical viewing cameras placed perpendicular to each other to access the top as well as the side view of the sample. The purpose of these cameras is to monitor the movement of the sample. A laser beam is used to identify the position of the X-ray beam falling on the sample and to bring the sample exactly at the focal point. Figure 1 shows the schematic diagram of 2D Micro-XRF setup (top view) along with the spectral profile of the bremsstrahlung radiation coming from the polycapillary tube. In an instrumental configuration with X-ray tube, followed by an X-ray filter, the bremsstrahlung hump gets eliminated and thus, we lose the benefits of the major intensity portion of the tube spectra.

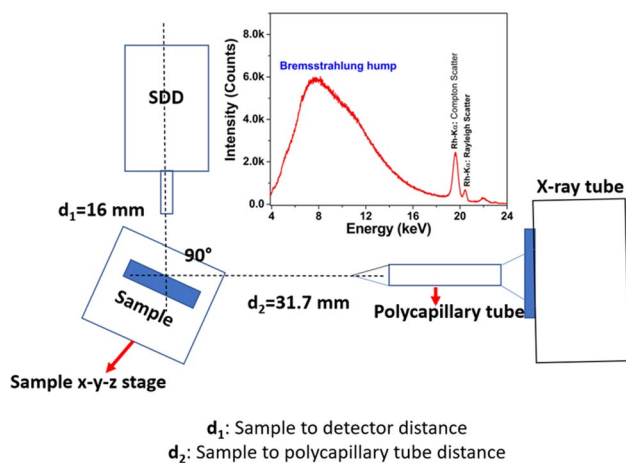


Fig. 1 Schematic diagram of 2D Micro-XRF setup (top view) along with the spectral profile of the bremsstrahlung radiation coming from the polycapillary tube

Utilization of X-ray tube without any X-ray filter results in improvement of the detection limits of the elements having absorption edges near the bremsstrahlung hump which was earlier shown in one of our studies [25]. It can be seen from Fig. 1 that the bremsstrahlung hump covers an energy region from 4 to 16 keV with maxima at 8 keV. So, all the elements e.g. Cr, Mn, Fe, Co, Ni, Cu, Mo having X-ray absorption edges around this energy region are excited most efficiently. Kunimura et al. demonstrated that in TXRF geometry, usage of polychromatic excitation improves the detection limit (2–3 times) compared to that obtained with monochromatic excitation with a low power X-ray tube as excitation source [22]. In the present study, we have used a low power X-ray tube (50 W), so direct polychromatic excitation is responsible to obtain good signal to background ratio. Though the background counts are very high when full bremsstrahlung beam is used; still due to very huge peak counts the detection limits have improved significantly.

For determination of elemental concentration, it is always better to do area scanning in order to avoid the error associated with the inhomogeneous distribution of elements in the steel matrix at a particular point/spot. If a large area i.e. $2 \times 2 \text{ mm}^2$ is scanned it will take care of this effect. Using micro-focused beam, an area scan of $2 \times 2 \text{ mm}^2$ was chosen for each sample with a step size of $100 \mu\text{m}$. Each spot was measured for 1 s. The total measurement time was 400 s for a single measurement. Each sample was measured in triplicate at three different positions. The sum spectra obtained were used for the analysis. Quantification of the analytes in the samples analyzed by μ -XRF technique involves deconvolution of the measured sum spectra for extracting the area under the curve. This deconvolution was performed using AXIL QXAS 3.6 as well as PyMca [26, 27]. The fitting of

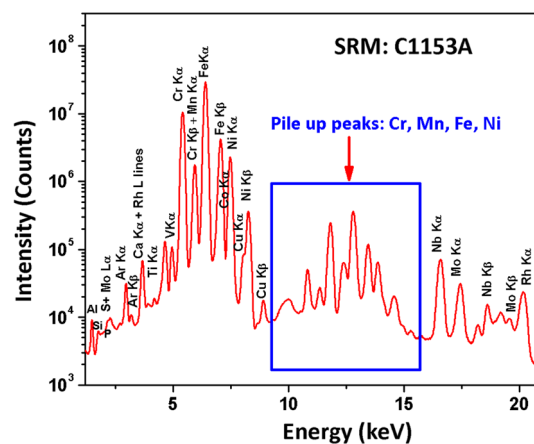


Fig. 2 Micro-XRF sum spectrum of SRM C1153A standard (measurement time 400 s)

the spectral data were performed by the least square fitting procedure by minimizing the χ^2 value.

Result and discussions

A typical micro-XRF sum spectrum of a steel standard (SRM: C1153A) is shown in Fig. 2. It can be seen from the spectrum that all the trace as well as major elements present in that standard are clearly visible. It can also be seen that the pile up peaks of Cr, Mn, Fe, and Ni are also present in that spectrum. The peak of Ar $K\alpha$ is coming from the air atmosphere. To determine area under each elemental lines; we have used fitting software PyMca [27]. To obtain a good fitting, we have divided the whole spectrum in two energy regions e.g. 1.3–2.5 keV for the fitting of elemental lines coming from low Z elements like Al, Si, P, S and 2.5–18 keV; for the fitting of elemental lines coming from medium and high Z elements. It can be seen from the Fig. 3a and b that all major as well as trace elements can be very well fitted using this program.

During the XRF measurements of low Z elements like Si, P, S there is one inherent limitation, which is low fluorescent yield. However, there are certain factors which could also improve the detection limits of low Z elements e.g. using low energy excitation source/line that is closer to the absorption edge of the elements of interest and use of vacuum atmosphere/He gas purging. Unfortunately, we do not have these facilities in our spectrometer. Although we have used air atmosphere during this work, however because of bremsstrahlung continuum excitation, both Rh $K\alpha$ as well as Rh $L\alpha$ excited the sample. Now, as Rh $L\alpha$ (2.69 keV) is closer to the absorption edge of Si (1.851 keV), P (2.157 keV) and S (2.485 keV); these elements will be excited efficiently. Also micro-focused beam with increased

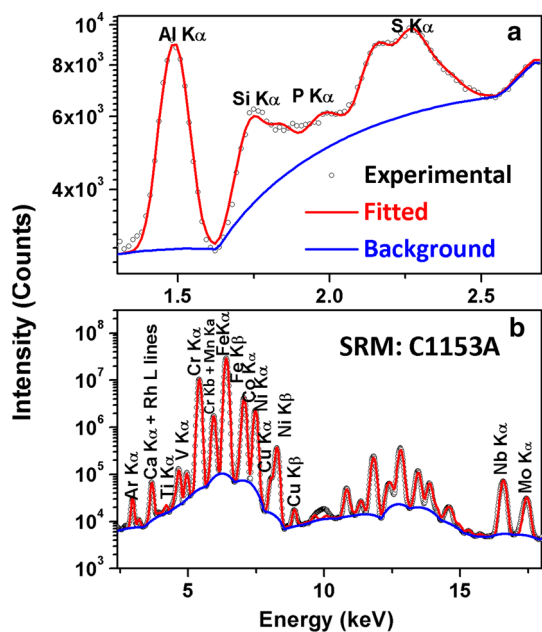


Fig. 3 PyMca fitted Micro-XRF spectra of SRM: C1153A standard in two different energy regions e.g. 1.3–2.5 keV (a) and 2.5–18 keV (b)

flux will improve the detection limits compared to conventional EDXRF [21]. There is a report where P is determined in EDXRF geometry in presence of He atmosphere [28], however there are also many work reported in the literature where elements like P, S are measured in air atmosphere by EDXRF [29, 30]. So keeping all these things in mind we felt that Si, P, and S can be measured in air atmosphere using a bremsstrahlung continuum where Rh $L\alpha$ can also excite all these elements efficiently.

In XRF geometry as the X-ray penetrates into the sample matrix; it suffers from huge matrix effect [31]. So to overcome this matrix effect we need some matrix matched calibration standards. In this work we have used six SRM standards of steel samples. These standards have different range of concentrations of trace as well as major elements. Now for each element present in the sample matrix, separate calibration curves were constructed. Figure 4 shows the calibration curve obtained for low Z elements Si, P and S and Fig. 5 shows the calibration curve for other elements (V, Cr, Mn, Co, Ni, Cu, Nb, Mo) present in those SRM standards. During the construction of calibration curve; we have normalized the total counts by dividing the elemental counts with the counts of Fe $K\alpha$; which is present as major element in steel samples. This methodology will ensure that if there are any changes in the count rates due to slight change in instrumental alignment or parameters; the count rates of Fe $K\alpha$ will also change accordingly. It can be seen from Figs. 4 and 5 that the calibration curves for each element are linear with correlation coefficient (0.98–0.99). Elements like P, S, V, Co and Mo were present in less than 1% concentration

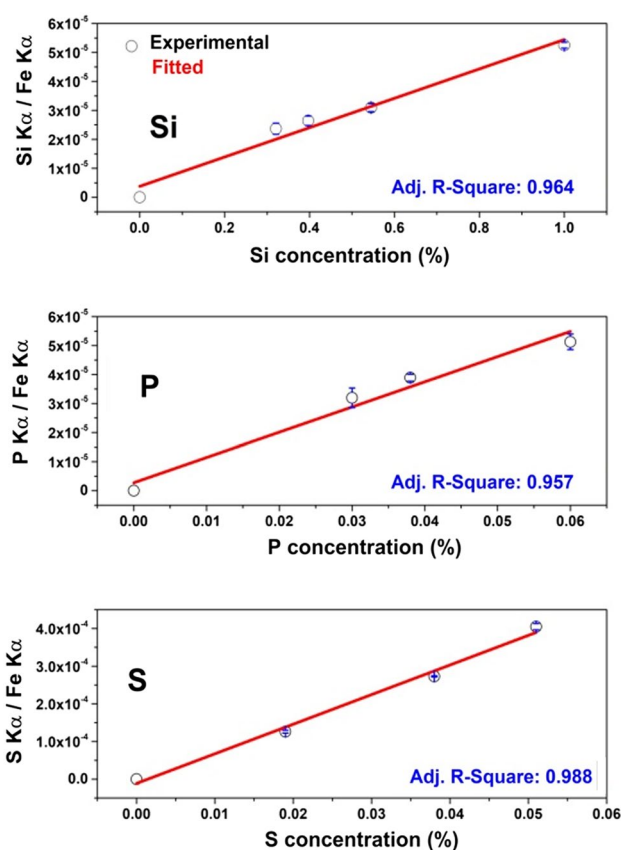


Fig. 4 Calibration curve obtained in micro-XRF geometry for low Z elements e.g. Si, S and P

level; still we have obtained linear calibration curves with good correlation coefficient (0.95–0.98).

The calibration curves, obtained for each element, were used to determine elemental concentrations (both major as well as trace) in two SRMs of steel. Table 1 shows the comparison of micro-XRF determined concentrations and certified concentrations of two standards of steels (SRM-1297 and SRM-1295). It can be seen from this table that there is an excellent agreement between micro-XRF determined concentrations and certified concentrations for not only major elements, but also for the trace elements like P, S, V, Cu, Mo. However, for Co the deviation is 30.5%, which could be due to the presence of huge Fe $K\beta$ peak (7.059 keV) that interferes severely with Co $K\alpha$ peak (6.925 keV). This leads to the poor analytical results for “Co” in SRM 1295. Further, in case of SRM 1297 this deviation is less for Co i.e. 16.5%. This is because in SRM 1297, Co is present in percentage level, so the effect of this interference of Fe $K\beta$ line is less as compared to in SRM 1295 where the concentration of Co is in ppm level only (~200 ppm). So, it can be seen that the developed micro-XRF based technique is capable of analyzing steel samples for a very wide concentration range starting from more than 10% to as low as 30 ppm.

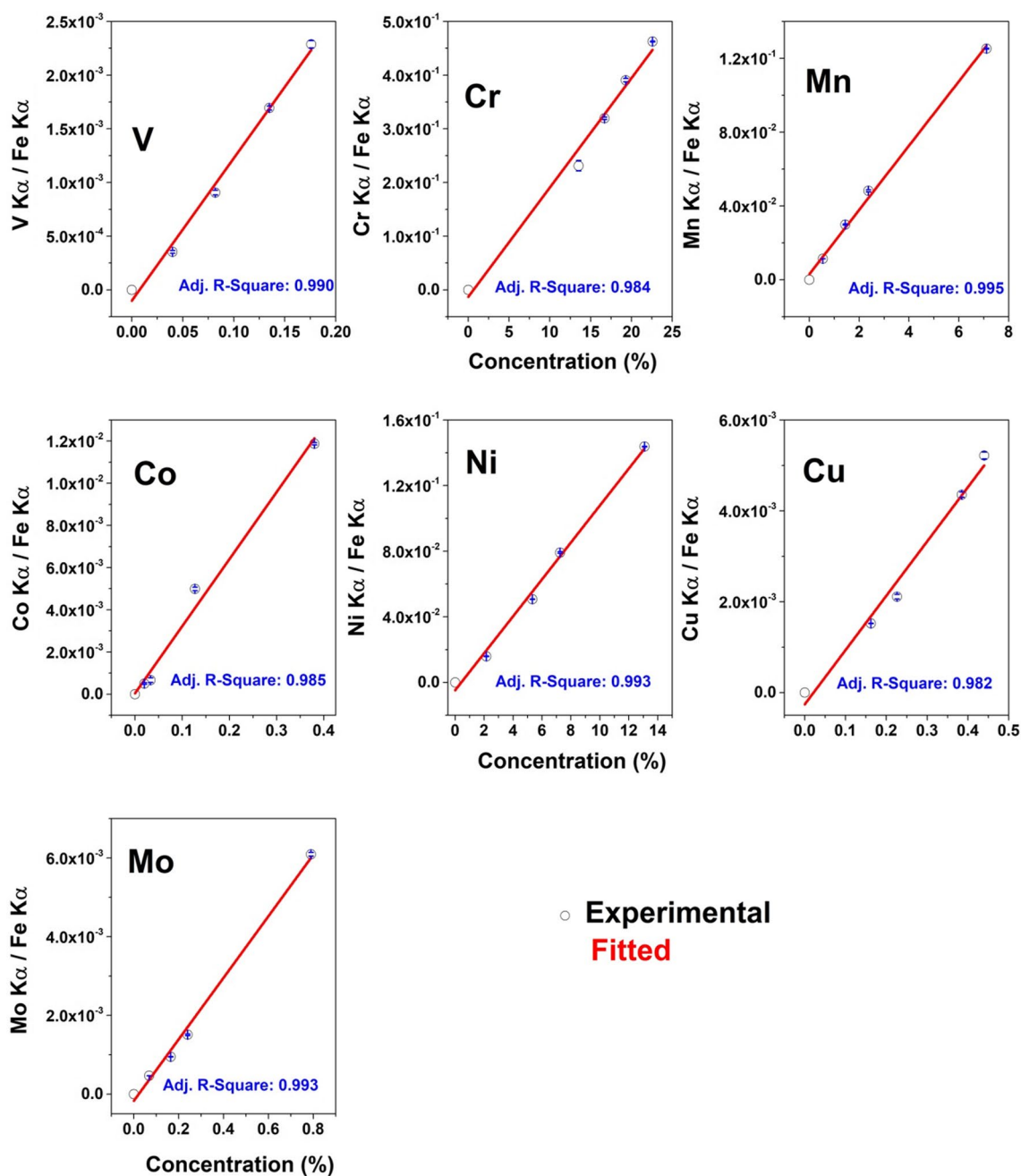


Fig. 5 Calibration curve obtained in micro-XRF geometry for medium and high Z elements

To compare the analytical results of our developed micro-XRF methodology with the reported values, we have gone through extensive literature reports related to the analysis of stainless steel samples using different EDXRF instruments. Pantazis et al. have shown that using the Hand Held XRF (HHXRF) spectrometer, stainless steel samples could be analyzed non-destructively for the determination of elements in percentage level [23]. However, it could not analyze the elements which are present down to ppm level. Moreover, elements like Si, P, S, and V could not be analyzed using

that spectrometer. There is also a report for the analysis of painted steel samples using HHXRF [24]. In that report also they have analyzed the major elements present in percentage level only. Based on the EDXRF results of the work reported by Tiwari et al. and Pantazis et al [23] we have compared the analytical parameters like deviation, RSD for different elements in steel matrix against our values which is shown in Table 2. From the table it can be seen that elements like Si, P, S, V, Mo and Co were not reported in both the studies. However, using our developed methodology, we

Table 1 Comparison of Micro-XRF determined concentrations and certified concentrations of two certified Standard Reference Materials of steel (SRM-1297 and SRM-1295)

Elements	SRM 1297 (SAE 201)		SRM 1295(SAE 405)		SS 304	
	Micro-XRF determined Conc	Certified Conc	Micro-XRF determined Conc	Certified Conc	Micro-XRF determined Conc	Reported Conc
Si	0.46±0.08 (%)	0.397±0.004 (%)	0.34±0.04 (%)	0.321±0.007 (%)	0.95±0.06 (%)	1 (%)
P	596±48 (ppm)	380±02 (ppm)	240±50 (ppm)	220±20 (ppm)	565±69 (ppm)	450 (ppm)
S	29±3 (ppm)	33±3 (ppm)	ND	3±2 (ppm)	154±51 (ppm)	150(ppm)
V	842±7 (ppm)	800±30 (ppm)	801±15 (ppm)	820±30 (ppm)	–	–
Cr	17.13±0.06 (%)	16.69±0.02 (%)	14.50±0.28 (%)	13.52±0.02	18.53±0.01 (%)	17.5–19.5 (%)
Mn	7.05±0.01 (%)	7.11±0.06 (%)	0.39±0.01 (%)	0.387±0.007 (%)	1.99±0.09 (%)	2(%)
Co	0.106±0.002 (%)	0.127±0.003 (%)	261±1 (ppm)	200±10 (ppm)	–	–
Ni	4.96±0.01 (%)	5.34±0.04 (%)	0.175±0.001 (%)	0.194±0.006 (%)	8.38±0.03 (%)	8–10.5(%)
Cu	0.391±0.001 (%)	0.442±0.008 (%)	0.230±0.001 (%)	0.260±0.006 (%)	–	–
Mo	0.316±0.002 (%)	0.331±0.008 (%)	186±3 (ppm)	230±20 (ppm)	–	–
Nb	79±15 (ppm)	<90 (ppm)	ND	<5 ppm	–	–
Sample description	Area scanned: 2×2 mm Dia: 32 mm, thickness: 19 mm		Area scanned: 2×2 mm Dia: 32 mm, thickness: 19 mm		Area scanned: 2×2 mm	

*ND: Not Detected, n=3, σ=1

could determine concentrations of these elements even at trace levels. For other major elements like Cr, Mn and Ni, the obtained accuracy and precision is comparable with the literature reported data. Further, there is no report showing the capability of XRF based non-destructive method for the analysis of both major as well trace elements down to such low concentration level, to the best of our knowledge. The developed Micro-XRF based technique is capable of determining both trace as well as major elements with good accuracy and precision non-destructively.

It is very important to determine the detection limit of this micro-analytical method for the trace analysis in stainless steel matrix. This will help us to get an idea up to how much lower concentration level; elemental analysis can be possible in these samples. So SRM 1151 was chosen as a

sample matrix to determine the detection limits of different elements present in it. For the determination of detection limits, same area scan procedure was used as mentioned in the experimental portion, only the counting time at each point was kept 2 s, so total measurement time was 800 s. The detection limit for each elements present in the steel sample was calculated using the following formula [32]:

$$DL = \frac{3 \times \sqrt{I_B}}{I_P} \times C_i$$

here I_B is the area under the background, I_P is the area of the peak of analytes line of interest and C_i is the concentration of the analyte. The detection limits obtained for different elements are shown in Table 3. There is a recent work done by

Table 2 Comparison of accuracy and precision obtained in this work for the determination of trace as well as major elemental concentrations in steel samples using EDXRF technique with literature reported values

Elements	Accuracy (in %)			Precision or RSD* (in %)		
	In this work	Tiwari et al. [10]	Pantazis et al. [23]	In this work	Tiwari et al.	Pantazis et al.
Si	13.70	ND	ND	17.4	ND	ND
P	36.24	ND	ND	8.1	ND	ND
S	–13.79	ND	ND	10.3	ND	ND
V	4.99	ND	ND	0.8	ND	ND
Cr	2.57	–2.05	0.27	0.4	2.1	1.4
Mn	–0.85	2.22	2.40	0.1	4.4	4.2
Co	–19.81	ND	ND	1.9	ND	ND
Ni	–7.66	–2.44	0.73	0.2	2.3	2.2
Cu	–13.04	–30.95	1.18	0.3	2.5	15.4
Mo	–4.75	ND	ND	0.6	ND	ND

Table 3 Comparison of detection limits of different elements obtained in stainless steel matrix (SRM: 1251 was used to calculate the detection limits) using the developed Micro-XRF based methodology with recently reported values using hand held XRF instrument as well as Micro-XRF instrumentation (matrices are different)

Elements	Detection limit (ppm)		
	This work	Krummenauer et al. [33]	Other micro-XRF**
Si	320.4	NA	352 [36]
P	52.2	NA	179 [36]
S	19.6	NA	53 [37]
V	14.5	30	28 [36]
Cr	13.1	60	30 [36]
Mn	15.4	250	19 [36]
Co	1.3	1000	–
Ni	14.5	130	–
Cu	7.6	50	–
Nb	24.9	10	–
Mo	10.8	10	–

**Matrices are different

Krummenauer et al. where a hand held XRF instrument was used to determine detection limits of different trace elements in steel alloy samples [33]. We have compared their reported detection limits with our values in Table 3. We haven't found any literature report where micro-XRF is used to analyze trace as well as major elemental concentrations in complex and important matrices like steel samples non-destructively except one work where chlorine was determined in painted steel samples using confocal Micro-XRF [34]. However there are some reports where Micro-XRF has been used for the analysis of ceramic samples or soil standards [35, 36]. We have compared the detection limits obtained using the conventional micro-XRF method with that obtained in our work in Table 3. It can be seen from the Table 3 that except Nb and Mo, the detection limits of all other elements like Cr, Mn, Co, Ni, Cu, etc. are much better using our developed Micro-XRF based methodology compared to that using handheld XRF spectrometer. In addition to that the detection limits of elements like Si, P, and S were in ppm level which could not be detected by their spectrometer. While, if we compare the detection limits reported for various elements like Si, S, P, V, Cr, Mn, Ni using conventional micro-XRF spectrometer in ceramic or soil matrices with our values, it can be seen that our detection limit is still better. Moreover, it has to be remembered that the detection limits we are reporting is in presence of heavy Z matrix like steel. However, the detection limits reported using other conventional micro-XRF were in low Z matrix like ceramics or soil samples. So it is quite interesting to achieve such low detection limit in Micro-XRF geometry in presence of such huge matrix. There are several reasons responsible for achieving

such low detection limits. The micro-focused beam optics allows ensuring utilization of the entire X-ray flux emitted from the X-ray tube, to excite the sample spot. While using a focused beam, the whole flux of the X-ray is falling on a very small area ($30 \times 30 \mu\text{m}$), so the effective excitation will be increased many times. Utilization of X-ray beam without any X-ray filters, results in improvement in the MDL values for the elements having absorption edges near the bremsstrahlung hump. The bremsstrahlung covers the energy region from 4 to 16 keV with maxima at 8 keV. So all elements having X-ray absorption edges in that region will be efficiently excited e.g. Cr, Mn, Fe, Co, Ni, and Cu. However, Nb and Mo have energies above 16 keV and were not excited so efficiently by the bremsstrahlung, so the detection limits of these two elements were poor. In addition to that using micro-focus geometry, the sample to detector distance is minimized. This increases the solid angle subtended by the detector, which enhances the counting statistics. All these factors cumulatively improve the excitation of the sample, which results into a very good counting statistics as well as analytical results. In conventional EDXRF spectrometers the above stated benefits cannot be obtained. All these aspects are discussed in detail in our previous work [21]. So this huge improvement in detection limit for different elements present in steel matrix using micro-XRF geometry allow us to determine elemental concentration at ppm level, which was previously not at all possible using XRF method.

The developed methodology was applied for the analysis of other important steel samples like D9 alloy, SS-304 which are used in different industries as well as in cladding materials of nuclear reactors. Figure 6 shows the fitted Micro-XRF spectrum of D9 alloy sample. The elemental concentrations obtained using the developed methodology was compared with the reported values and presented as bar diagram in Fig. 7. It can be seen from this figure that the elemental concentrations obtained using the developed Micro-XRF based technique are in agreement with the reported values. Similarly, the developed method was also applied for the nondestructive analysis of SS 304 alloy and the results are shown in Table 1 which shows comparison of Micro-XRF determined elemental concentration with the reported value for SS304 alloy sample. It can be seen that the results obtained using the developed methodology are in agreement with the reported data.

The outcomes from all these validation studies clearly demonstrate that the developed micro-XRF based methodology has immense potential for the non-destructive analysis of different types of steel samples. This is a substantial improvement compared to previously reported data where to determine elemental concentrations in steel at such low level concentrations require dissolution as well as matrix separation [15]. It has been observed that using micro-focus beam in combination with bremsstrahlung continuum excitation

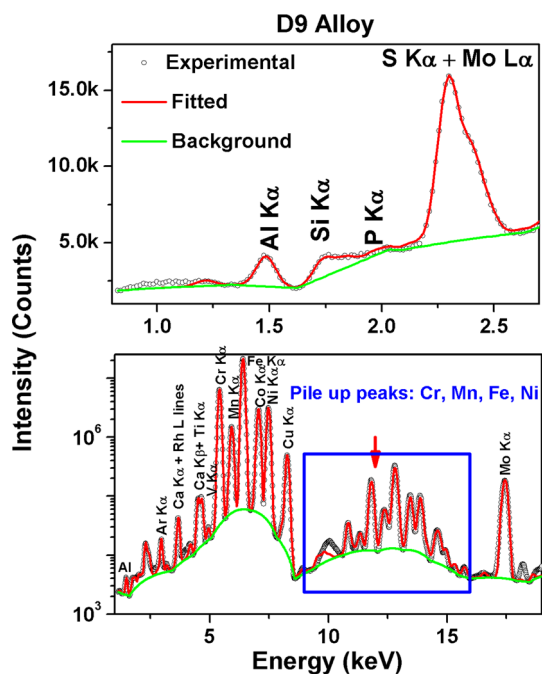


Fig. 6 PyMca fitted Micro-XRF spectra of D9 alloy at two different energy regions e.g. 1.3–2.5 keV (A) and 2.5–18 keV (B)

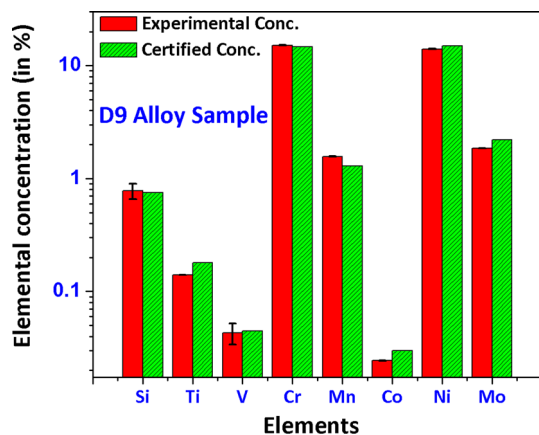


Fig. 7 Comparison of micro-XRF determined elemental concentrations present in D9 alloy sample with the reported values

improves the detection limit as well counting statistics substantially compared to conventional EDXRF geometry. However all these studies were done in thin film specimen, where a few micro-litre of sample was deposited on a thin transparent scotch tape. While using a thick as well as very complex matrix system like steel, the scenario will be completely different, where there is a huge matrix effect as well as scattering. Due to these limitations, in earlier papers people have used normal EDXRF or hand held XRF for the determination of elements that are present in percentage (0.1–20%)

level only. For determination of trace elements (by XRF/ TXRF) which are present in ppm level; the sample needed to be dissolved and the major matrix has to be separated, which is very tedious job. In this work we have utilized the micro-XRF geometry to determine elements which are present in ppm level also without any dissolution or any sample pretreatment. This will save lot of time and efforts. This type of approach opens up many possibilities for the nondestructive analysis down to ppm level in different types of sample matrices e.g. geological samples, or alloy samples. This is the novelty of this work. Moreover the developed method required negligible running cost as there is no need of any gas flow or liquid nitrogen supply, plasma etc. The presently developed methodology does not require any big facilities like neutron source/proton source which are essential for NAA and PIGE, respectively.

Conclusions

A very simple nondestructive method has been developed for the determination of concentrations of major as well as trace elements present in various types of industrial stainless steel samples using XRF based technique. The full utilization of bremsstrahlung excitation in combination with micro-focused geometry improves the detection limits down to ppm level. This allows trace determinations down to ppm levels for different elements like Si, P, S, V, Co, Nb, Mo, etc., which were previously not possible. The developed methodology was validated using SRMs of stainless steel as well as some industrial steel samples. The analytical results obtained are very much satisfactory with good accuracy and precision. The nondestructive methodology developed in this work reduces the cumbersome dissolution process. Moreover, the developed methodology is simple, cost-effective which made it an ideal technique to be used for routine analysis of industrial steel samples for both major as well as trace determinations. This type of approach opens up many possibilities for the nondestructive analysis down to ppm level in different types of sample matrices including geological or alloy samples.

Acknowledgements The authors are thankful to Dr. P.K. Pujari, Director, Radiochemistry and Isotope Group and Dr. S. Kannan, Associate Director, Radiochemistry and Isotope Group and Head, Fuel Chemistry Division, for their support in this work. The authors would also like to thank Dr. Rajesh V. Pai, Head Fuel Development Chemistry Section, Fuel Chemistry Division for his keen interest and encouragement for this work. We are also thankful to Dr. Arnab Sarkar for providing the Standard Reference Materials of steel samples.

Declarations

Conflict of interest There is no conflict of interest to declare.

References

1. V. Karki, M. Singh, *Int. J. Mass Spectrom.* **421**, 51–60 (2017)
2. S. Mannan, S. Chetal, B. Raj, S. Bhoje, *Trans. Indian Inst. Metals* **56**(2), 155–178 (2003)
3. M. Montemor, M. Ferreira, N. Hakiki, M.D.C. Belo, *Corros. Sci.* **42**(9), 1635–1650 (2000)
4. C.-H. Yang, S.-J. Jiang, *Spectrochim. Acta, Part B* **59**(9), 1389–1394 (2004)
5. E. Cincu, I. Manea, V. Manu, D. Barbos, O. Sima, I. Gustavsson, P. Vermaercke, N. Vajda, Z. Molnar, H. Polkowska-Motrenko, *J. Radioanal. Nucl. Chem.* **274**(1), 199–205 (2007)
6. R. Nadkarni, B. Haldar, *Anal. Chim. Acta* **42**, 279–284 (1968)
7. S. Kashiwakura, K. Wagatsuma, *Isij International, ISI-JINT-2019-2549* (2020)
8. B. Kanrar, K. Sanyal, N. Misra, S. Aggarwal, *Spectrochim. Acta, Part B* **101**, 130–133 (2014)
9. S. Dhara, K. Sanyal, N.L. Misra, *Anal. Sci.* **19**, 196 (2019)
10. M. Tiwari, A. Singh, K. Sawhney, *Bull. Mater. Sci.* **24**(6), 633–638 (2001)
11. C. Lee, S. Roh, C. Lee, S. Hong, *Mater. Chem. Phys.* **207**, 91–97 (2018)
12. K. Suzuki, S. Ban-Ya, M. Hino, *ISIJ Int.* **41**(8), 813–817 (2001)
13. J. Brooks, F. Lambert Jr., *Weld. J.* **57**(5), 139s–143s (1978)
14. R. Klockenkämper, *Total reflection X-ray fluorescence analysis* (Wiley-Interscience, 1997)
15. G. Pepponi, P. Wobrauschek, C. Strelti, N. Zöger, F. Hegedüs, *X-ray Spectrom.* **30**(4), 267–272 (2001)
16. K. Sanyal, A. Khooha, G. Das, M. Tiwari, N. Misra, *Anal. Chem.* **89**(1), 871–876 (2016)
17. B. Kanrar, K. Sanyal, S. Dhara, *Spectrochim. Acta Part B: At. Spectrosc.* **177**, 106063 (2021)
18. K. Nakano, K. Akioka, T. Doi, M. Arai, H. Takabe, K. Tsuji, *ISIJ Int.* **53**(11), 1953–1957 (2013)
19. S. Fitzgerald, *Archeometriai Műhely* **3**, 75–80 (2008)
20. K. Nakano, C. Nishi, K. Otsuki, Y. Nishiwaki, K. Tsuji, *Anal. Chem.* **83**(9), 3477–3483 (2011)
21. K. Sanyal, B. Kanrar, S.D. Lenka, J. Anal. At. Spectrom. **36**, 803–812 (2021)
22. S. Kunitamura, J. Kawai, *Analyst* **135**(8), 1909–1911 (2010)
23. T. Pantazis, J. Pantazis, A. Huber, R. Redus, *X-ray Spectrom.* **39**(2), 90–97 (2010)
24. H. Ida, T. Segawa, S. Tohyama, J. Kawai, *Spectrochim. Acta, Part B* **60**(2), 249–252 (2005)
25. K. Sanyal, B. Kanrar, S. Dhara, J. Anal. At. Spectrom. **36**(4), 803–812 (2021)
26. B. Vekemans, K. Janssens, L. Vincze, F. Adams, P. Van Espen, *X-ray Spectrom.* **23**(6), 278–285 (1994)
27. V. Solé, E. Papillon, M. Cotte, P. Walter, J. Susini, *Spectrochim. Acta, Part B* **62**(1), 63–68 (2007)
28. S. Peräniemi, J. Vepsäläinen, H. Mustalahti, M. Ahlgrén, *Freseenius J. Anal. Chem.* **344**(3), 118–122 (1992)
29. V. Adya, A. Sengupta, S. Thulasidas, V. Natarajan, *At. Spectrosc.* **37**, 19–24 (2016)
30. X. Zhang, Q. Shan, Y. Liu, J. Shao, Y. Ling, D. Hei, W. Jia, *Appl. Radiat. Isotop.* **167**, 109436 (2021)
31. E.P. Bertin, *Principles and practice of X-ray spectrometric analysis* (Springer Science & Business Media, 2012)
32. K. Sanyal, B. Kanrar, N. Misra, M. Czyzycki, A. Migliori, A. Karydas, *X-ray Spectrom.* **46**(3), 164–170 (2017)
33. A. Krummenauer, P. Dias, H. Veit, Presented at the Journal of Physics: Conference Series, 2021 (unpublished)
34. R. Yagi, K. Tsuji, *X-ray Spectrom.* **44**(3), 186–189 (2015)
35. D. Papadopoulou, G. Zachariadis, A. Anthemidis, N. Tsirliganis, J. Stratis, *Talanta* **68**(5), 1692–1699 (2006)
36. K. Uhler, M. Griesser, G. Buzanich, P. Wobrauschek, C. Strelti, D. Wegrzynek, A. Markowicz, E. Chinea-Cano, *X-ray Spectrom.* **37**(4), 450–457 (2008)
37. T. Nakazawa, K. Tsuji, *X-ray Spectrom.* **42**(5), 374–379 (2013)